

GRZEGORZ PACH^{1*}

THE INFLUENCE OF ALTERNATIVE CHARACTERISTICS OF THE VICINITY OF THE VENTILATION DISTRICT ON AIR QUANTITY

Subnetwork with two nodes shared with entire ventilation network can be separated as its part. For the network under common ventilation conditions, one of these nodes will become the subnetwork starting node, while the other will be the subnetwork end node. According to the graphs theory, such a piece of the network can be considered as a subgraph of the graph representing the entire ventilation network. A special feature of that subgraph is lack of predecessors of the subnetwork starting node and lack of successors of the subnetwork end node. Ventilation district of a mine may be often treated as a subnetwork. Vicinity is a part of the network which is not separated as subnetwork. In the case of a ventilation district its vicinity forces air flow through the district. The alternative characteristic curve of the vicinity can therefore be compared to the characteristics curve of a fictional fan that forces the airflow in the district.

The alternative characteristics (later in the text: the characteristics) of the vicinity of the ventilation district in an underground mine strongly influence air quantity and therefore play a crucial role in the reduction of methane, fire and thermal hazards. The role of these characteristics and proper selection of their approximating function were presented in the article.

The reduction of resistance of an intake stopping (having influence on entire resistance of a ventilation district) produces increased airflow in the district. This changes of airflow in the district caused by a variation in internal resistance (e.g. by opening an internal regulation stopping) depends on the characteristic of the vicinity of the district. Proper selection of its approximating function is also important for this matter.

The methods of determination of the alternative characteristic curve of the district vicinity are presented. From these procedures it was possible to obtain the results of air quantities and differences in isentropic potentials between an inlet and an outlet to/from the ventilation district. Following this, the characteristics were determined by graphic and analytic methods. It was proved that, in contrast to flat vicinity characteristics, steep ones have a smaller influence on the airflow modification in the district (which are caused by a regulation of the district resistance). The characteristic curve of the vicinity determines the ability to regulate air quantity and velocity in the district.

Keywords: mine ventilation network, ventilation district, alternative characteristics, ventilation hazards

¹ SILESIAAN UNIVERSITY OF TECHNOLOGY, FACULTY OF MINING, SAFETY ENGINEERING AND INDUSTRIAL AUTOMATION, 2 AKADEMICKA STR., 44-100 GLIWICE, POLAND

* Corresponding author: grzegorz.pach@polsl.pl



© 2020. The Author(s). This is an open-access article distributed under the terms of the Creative Commons Attribution-NonCommercial License (CC BY-NC 4.0, <https://creativecommons.org/licenses/by-nc/4.0/deed.en>) which permits the use, redistribution of the material in any medium or format, transforming and building upon the material, provided that the article is properly cited, the use is noncommercial, and no modifications or adaptations are made.

1. Introduction

Considering natural hazards, mining ventilation is an important part of their mitigation (Szlązak & Kubaczka, 2012; Knechtel, 2011; Zhong et al., 2003; Szlązak et al., 2013; Liu et al., 2017; Yueze et al., 2017). The articles (Szlązak et al., 2018a; 2019) presented the influence of a ventilation system of the exploitation area on the methane hazard. Deeper and more intense mining causes higher methane emissions, including possible rock and methane outburst (Wang et al., 2019) and increased temperatures. These emissions and thermal hazards occur in every mining region in the world (Yuan et al., 2010; Uszko, 2009; Szlązak, 2018b). They have a significant impact on mining costs and safety (including required methane drainage, methane detection, air conditioning, etc.). (Hudeček et al., 2013; Nguyen et al., 2009; Szlązak et al., 2013; Drenda et al., 2016; Jeswiet & Szekeres, 2016). Therefore, sufficient air quantity in the district is essential to reduce these kinds of hazard (Koptoń & Wierziński, 2014; Drenda et al., 2018). According to Krausego (Krause & Smolinski, 2013) air quantity in a longwall should be considered as third important factor influencing methane hazard. Therefore knowledge taken from numerical computing about air quantity and methane amount in excavations is crucial (Yueze et al., 2017; Tutak & Brodny, 2018; Wang et al., 2016).

Entire ventilation network consists of several ventilation districts. A variation in the aerodynamic resistance in a district leads to modification of the resistance in the whole network. It modifies air quantity (Luo et al., 2014; Kolarczyk, 2008). So, air flows in ventilation networks may be sensitive to the change in air resistance (Semin & Levin, 2019) However, it is impossible to avoid these changes completely. They are caused by a change in excavation distances, by placement new machinery, clamping of excavations, rock slides etc. The mining ventilation system should be resistant to these changes (Luo et al., 2014; McPherson, 1993; Cheng et al., 2012). However, even a small change in the air resistance of a stopping results in a variation of airflow rate in the branches (Dziurzyński et al., 2017). In addition, adding a subsurface main fans station, changes airflow rates in a ventilation network (Szlązak et al., 2017).

Considering methane emissions and thermal hazards, the high resistance of the system enables sufficient air quantity to be maintained during excavations (Luo et al., 2014; Drenda et al., 2016), independently of the changes described.

The characteristics of a vicinity are useful for analysis of the system resistance (Kolarczyk et al., 2005; Kolarczyk et al., 2006). Knowledge of the characteristics allows us to determine the variation in air quantity as a result of different variations in ventilation district resistance. It simplifies computing of the system resistance for a ventilation engineer. The existing software that is available to engineers requires a lot of measurements and step by step trials to determine the network solution. The method described is simpler.

2. Background – the ventilation district and its vicinity

To carry out the research following assumptions were adopted:

- the airflow in branches is treated as one-dimensional,
- air density is constant,
- only steady-state of airflow are considered,
- there are no additional sources forcing the airflow through a ventilation network, such as Natural Ventilating Pressure.

Each branch in a ventilation network has its starting and ending node (w_p and w_k). It is possible to give two kinds of characteristics for this case:

- for passive branches, (constant air density), (McPherson, 1993):

$$\Delta W = f(V), \quad \Delta W = R \cdot V^2 \quad (1)$$

- for active branches (branches including fan), (Kolarczyk, 2008)

$$H = f(V) \quad (2)$$

where:

- V — air quantity in a branch with fan,
- ΔW — head loss,
- H — fan pressure,
- R — aerodynamic resistance in a branch.

It is possible to districtalize the group of linked branches and create an entire ventilation district (subnetwork) (Fig. 1) where node 1 is an inlet and node 14 is an outlet (Kolarczyk et al., 2005).

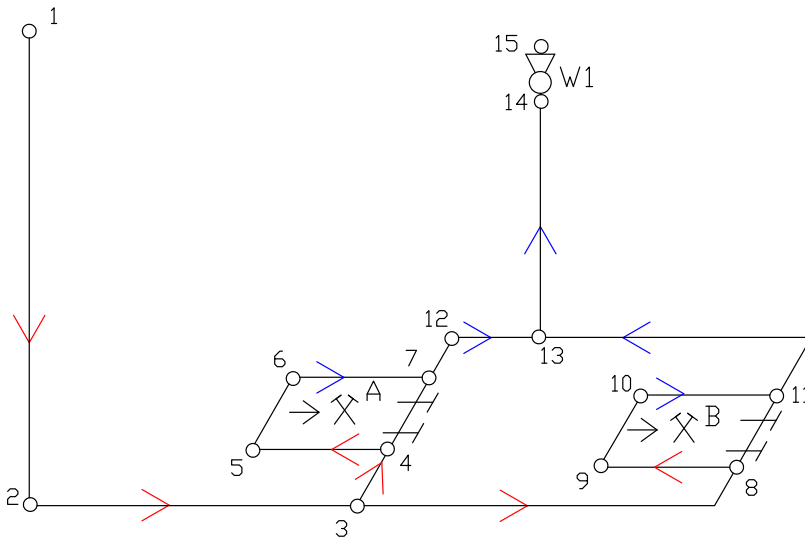


Fig. 1. Three-dimensional output schematic of “X” mine. An example of A and B ventilation districts

In this example, there are only passive branches, therefore the entire network is passive (Madeja-Strumińska & Strumiński, 2004). Thus, the characteristic of the district can be given by equation (1). The resistance R depends on the particular resistances of internal branches.

It is possible to form other districts. District A (Fig. 1) is one of the examples. It consists of the following branches (according to nodes): 3-4, 4-5, 5-6, 6-7, 4-7, 7-12. No. 3 is an inlet node. No. 12 is an outlet node. The rest of the branches create the vicinity of this district. A canonical diagram (Bystroń, 1956) of the X mine and the creation of the district is presented in Fig. 2. The dotted line in Fig. 2a links nodes 15 and 1. It is defined as “the atmosphere” branch.

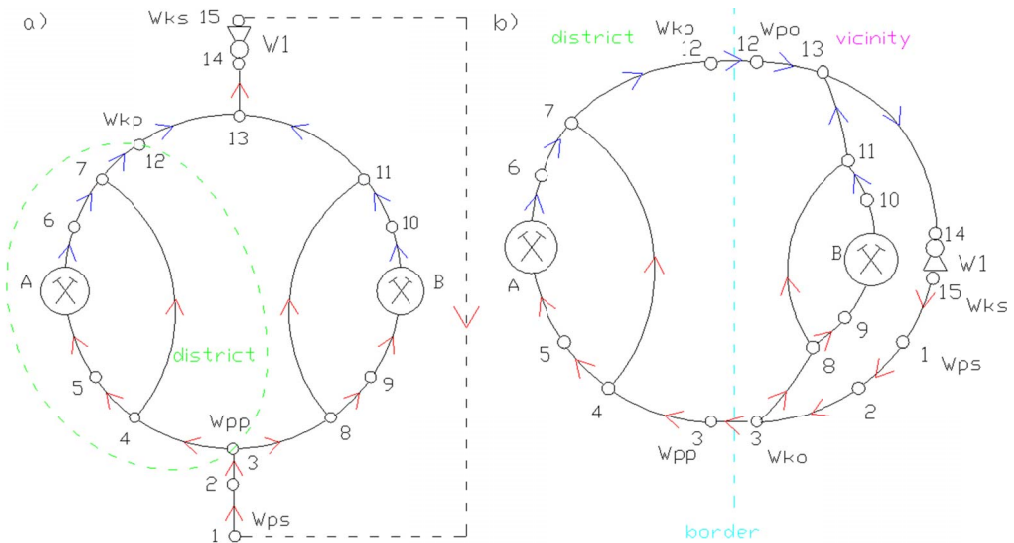


Fig. 2. The canonical diagram (a) and creation of the district and vicinity in a ventilation network (b).
 w_{ps} , w_{ks} – inlet and outlet nodes of the network; w_{pp} , w_{kp} – inlet and outlet nodes of the district;
 w_{po} , w_{ko} – inlet and outlet nodes of the vicinity

It must be noticed that after creation of the district (Fig. 2b), nodes 3 and 12 become linking nodes between the district and the vicinity. Node 3 is the inlet of the district w_{pp} and the outlet for vicinity w_{ko} . Node 12 is the outlet for the district and the inlet for the vicinity. In this case the district is the air collector and the vicinity forces the air flow. According to this dual action of the district – vicinity system, it can be compared to the dual action between a fan and a network. Both the district and the vicinity have one inlet and one outlet node, and so it is possible to determine the characteristics of the district (equation 3). It is sufficient for the passive element (equation 1).

$$\Delta W_z = f(V_z) = R_z \cdot V_z^2 \quad (3)$$

It is also possible to determine the characteristics of the vicinity (equation 4), which should be treated as the element forcing the flow (equation 2).

$$H_z = f(V_z) \quad (4)$$

Applying Kirchoff's second law (Hartman et al., 1997), it can be stated that in the operating point of a district – vicinity system, the head loss ΔW_z in the subnetwork equals the alternative increase of head H_z in the vicinity (Fig. 3).

$$\Delta W_z = H_z \quad (5)$$

Given Kirchoff's first law (Hartman et al., 1997), there pertains the following rule for linking nodes between the district and the vicinity: air quantity flowing in to the district equals air quantity flowing out of the vicinity and, analogously, the air quantity flowing out of the district equals air quantity flowing in to the vicinity.

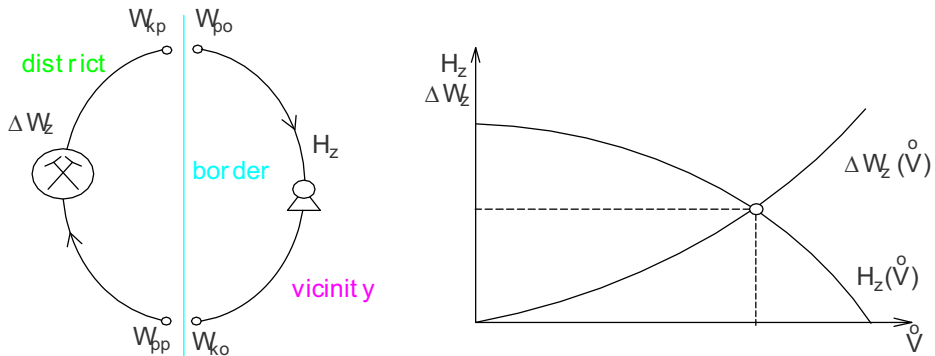


Fig. 3. Alternative characteristics of the section $\Delta W_z(V_z)$ and of the vicinity $H_z(V_z)$

The relationships obtained are useful for determination of the vicinity characteristics. These will be presented in the following districts.

3. Methodology – determination of the characteristics of the vicinity

Determination of the characteristics of the vicinity given in Fig. 2b is not a problem. Connections in parallel and in series enable the problem to be solved by, for instance, the graphical method. However, in the cases of real mines there are many cutsets, which don't permit this method to be used (Krach, 2014).

The characteristics of the vicinity can be determined by variations in the resistance of branches and further measurements of air quantity (where possible) (Kolarczyk et al., 2005). The algorithm is as follows:

a) “In-situ” measurements

1. Set several changes in resistance by opening and closing of internal stoppings. This leads to several variants of air distribution inside the district.
2. Measure the air quantity (V_z) at the inlet and/or the outlet of the district for each variant from the first point of the algorithm.
3. Determine the isentropic potentials (Bystroń, 1999) for inlet node w_{pp} and outlet node w_{kp} to/from the district.
4. Determine the difference in potentials $\Delta\Phi$ between these nodes. This difference equals the alternative head loss ΔW_z in the district, and thus in its vicinity. It can be described by equation 6:

$$\Delta\Phi = \Delta W_z = H_z \quad (6)$$

5. Having alternative values of V_z and an alternative head increase H_z for several measuring and computing variants, it is possible to determine and to draw the characteristic of the vicinity (Fig. 3).

b) Numerical simulations

Analogous operations (1-5) can be undertaken having a mathematical model of a network. (Kolarczyk et al., 2005). The air distribution is obtained by changing the branch resistance (in a district) (Gillies et al., 2004) and further numerical simulations.

In practice, both methods (a and b) are commonly used.

4. The analysis of the impact of the alternative characteristic curve on the district's ventilation

The role of alternative characteristics of vicinity on air quantity in a district was presented in three examples.

Assumptions. Numerical simulations were done for steady-states in passive networks (with constant density), for one directional and turbulent flow and without additional sources forcing the air through the ventilation network, such as Natural Ventilating Pressure (Kolarczyk, 1993).

According to research undertaken (Kolarczyk et al., 2005), the characteristics of a vicinity can be approximated by a linear function:

$$H_z = a \cdot V_z + b \quad (7)$$

or a parabolic function:

$$H_z = a \cdot V_z^2 + b \cdot V_z + c \quad (7a)$$

where a , b and c depend on the resistance of branches, the structure of vicinity and the curves of those fans which are in the vicinity of a district. The influence of the a and b coefficients on proper air quantity in a mining district will be discussed in the next section.

The first example refers to an approximation by linear and parabolic function when the characteristics are almost similar (convergent). The second example refers to opposite situation when the characteristics are not convergent. The third example is about the role of characteristics inclination on air quantity in a ventilation district.

The examples

Example 1. A longwall "C" in the "S" coal mine has a "U-tube" ventilation system and re-treating mining system. The characteristic of the vicinity was determined according to the method presented in the previous chapter (the violet curve in Fig. 4). The equation can be written as (8):

$$H_z = -0.1263 \cdot V_z^2 - 16.436 \cdot V_z + 498.7 \quad (8)$$

The resistance of the district is 1.5495 kg/m^7 (simple parallel and in-series connections, see Fig. 4 – green line). Equations 3, 5 and 8 enabled formulation of a system of equations for determination of the alternative air quantity V_z . This was determined to be $13.03 \text{ m}^3/\text{s}$ ($782 \text{ m}^3/\text{min}$). The alternative head loss in the district is 263 Pa. The results are similar to the results based on "in-situ" measurements (a variant without a change in the resistance of the branches in the mining district). It proves that the characteristic of the vicinity was selected appropriately (equation 8).

Approximation for the same vicinity was done with application of the linear function. The following formulae (9) was determined (blue line in Fig. 4):

$$H_z = -22.561 \cdot V_z + 557 \quad (9)$$

For the same alternative resistance $R_z = 1.5495 \text{ kg/m}^7$ air quantity was $V_z = 13.03 \text{ m}^3/\text{s}$ ($782 \text{ m}^3/\text{min}$) and the increase of alternative head loss $H_z = 263 \text{ Pa}$. Thus, the results were similar to those which were achieved with the second degree polynomial approximation.

Next, it was assumed that airflow should be increased (e.g. according to increased methane emissions).

The first step was to open the district stoppings, and then it led to decrease of district resistance up to 0.47 kg/m^7 (Fig. 4 – red curve). As for the effect this achieved:

- for the second degree polynomial approximation – an increase of air quantity V_z in the district (at the inlet) up to $18.25 \text{ m}^3/\text{s}$ ($1095 \text{ m}^3/\text{min}$) and a decrease of alternative head loss to 156.6 Pa .
- for the linear approximation – an increase of air quantity $17.96 \text{ m}^3/\text{s}$ ($1078 \text{ m}^3/\text{min}$) and head loss 151.6 Pa .

The results indicate that the two methods of approximation gave a small difference between the obtained air quantities and head loss ($0.29 \text{ m}^3/\text{s}$ and 5 Pa). Looking at Fig. 4 it can be observed that the district vicinity curves (blue and violet lines) are similar within the area of the diagram, therefore any variation of district resistance R_z gives similar V_z and H_z for the linear as well as for the second stage polynomial approximation. However, it is not true for every vicinity characteristic. This is confirmed in Example 2.

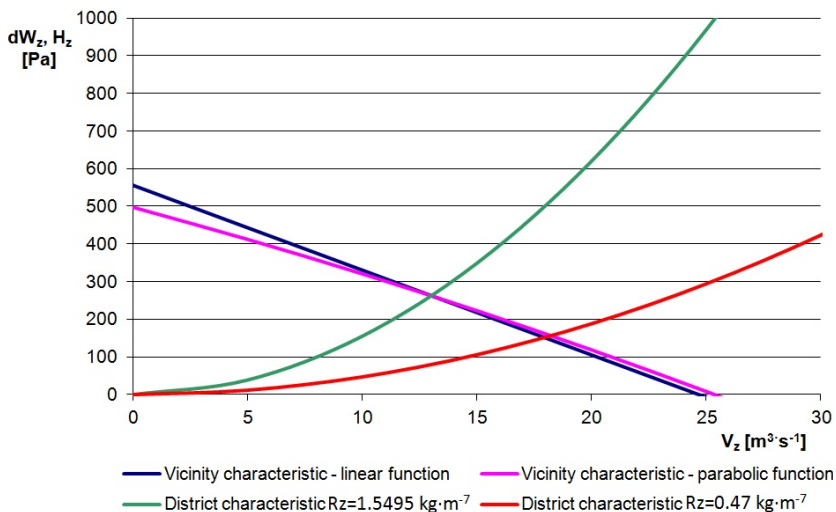


Fig. 4. The vicinity and ventilation district characteristics – Example 1

Example 2. The ventilation district “Y” in “P” coal mine had a stopping at the inlet. It gave a high value of resistance $R = 8.463 \text{ kg/m}^7$ (Fig. 5 – green line). The air quantity V_z was $6.67 \text{ m}^3/\text{s}$

(400 m³/min). The characteristic of the vicinity was obtained based on seven computed (PC) variants of air distribution (achieved by different setups of intake stopping). It gave the following equations for the vicinity characteristic:

- parabolic function approximation (Fig. 5 – violet line)

$$H_z = -0.712 \cdot V_z^2 - 16.892 \cdot V_z + 521.32 \quad (10)$$

- linear approximation (Fig. 5 – blue line)

$$H_z = -14.524 \cdot V_z + 473.8 \quad (11)$$

After total opening of intake stopping the alternative resistance of the district decreased to $R = 0.8 \text{ kg/m}^7$ (Fig. 5 – red line). The alternative air quantity V_z was determined for the values of R and H_z . It gave:

- the characteristic determined by the parabolic function – $V_z = 13.80 \text{ m}^3/\text{s}$ (828 m³/min), $H_z = 152 \text{ Pa}$ (Fig. 5 – the intersection of red and violet lines)
- the characteristic determined by the linear function – $V_z = 16.89 \text{ m}^3/\text{s}$ (1013 m³/min), $H_z = 228 \text{ Pa}$ (Fig. 5 – the intersection of red and blue lines).

It can be observed that the two different kinds of approximation gave a marked discrepancy in the results (about 20% for air quantity V_z and above 30% for the increase in alternative head loss H_z). After additional simulations of air distribution across the entire mine, it turned out that setting the ventilation district resistance at 0.8 kg/m^7 should produce values for V_z and H_z close to those which were achieved by parabolic approximation. The example shows that the parabolic function produces a better matching of the characteristic. This is crucial, especially when two vicinity characteristics deviate markedly (Fig. 5).

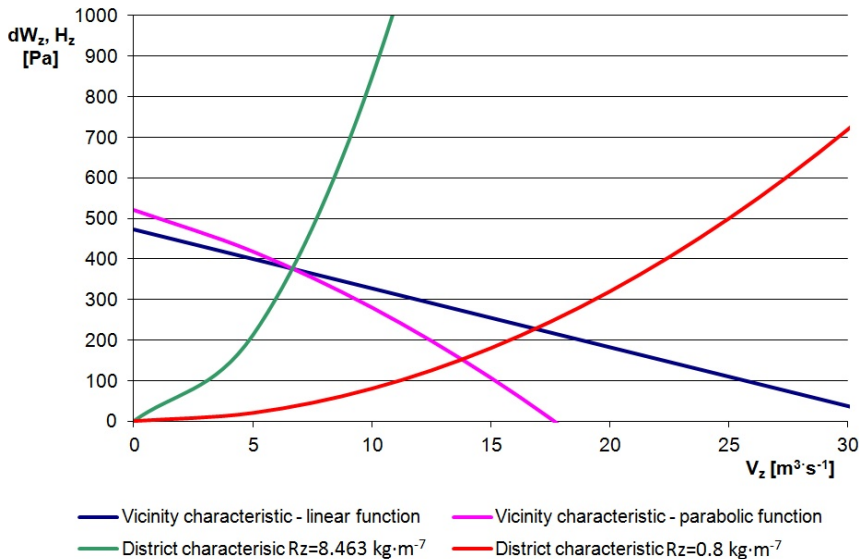


Fig. 5. The characteristics of the vicinity and ventilation district – example 2

Example 3. This example refers to the influence of vicinity characteristics curve on the ability of air quantity regulation. A very steep characteristic was assumed (compared to the characteristic obtained by linear approximation in example 1, Fig. 6, blue line):

$$H_z = -50 \cdot V_z + 914.495 \quad (12)$$

The value of the b coefficient was set to obtain the intersection of the vicinity characteristic and the operating point of the district – vicinity system, similar to example 1 – (coordinates $V_z = 13.03 \text{ m}^3/\text{s}$ and $H_z = 263 \text{ Pa}$). Looking at Fig. 6 it is the intersection of three lines. The violet line in Fig.6 is merely for comparison. In fact, it is the vicinity characteristic from example 1. The resistance was assumed to be the same as for example 1 $R_z = 1.5495 \text{ kg/m}^7$, the green line in Fig. 6. To obtain a the same air quantity $V_z = 17.96 \text{ m}^3/\text{s}$ (analogous to example 1) the district resistance should be reduced to 0.05 kg/m^7 . It means a decrease of 0.42 kg/m^7 (compared to example 1, equation 9). Such a marked reduction might not be possible, due to the resistance values of neighboring branches. The reduction to 0.47 kg/m^7 (Fig. 6 – red line) would give air quantity of $15.91 \text{ m}^3/\text{s}$. It is worth recalling that for the flat vicinity characteristic the air quantity would be $17.96 \text{ m}^3/\text{s}$.

The internal loss of air was assumed to be 20% (through internal stoppings) and the cross-sectional area of the longwall face was 12 m^2 . For intake air quantity $V_z = 13.03 \text{ m}^3/\text{s}$ (closed stopping – initial state) air velocity in the longwall is 0.87 m/s . The opening of the stopping gave:

- for a flat vicinity characteristic (violet line – Fig. 6), a velocity increase of 1.20 m/s ,
- for a steep vicinity characteristic (blue line – Fig. 6), a velocity increase of 1.06 m/s .

Example 3 shows that in comparison to the steep vicinity characteristic (equation 12 – Fig. 6 blue line), a flatter curve (equation 9, Fig. 6, violet line) allows a larger air quantity to be supplied under the same change of stopping resistance. It should also be mentioned that the initial operating point of district – vicinity system was the same for both cases (the intersection point

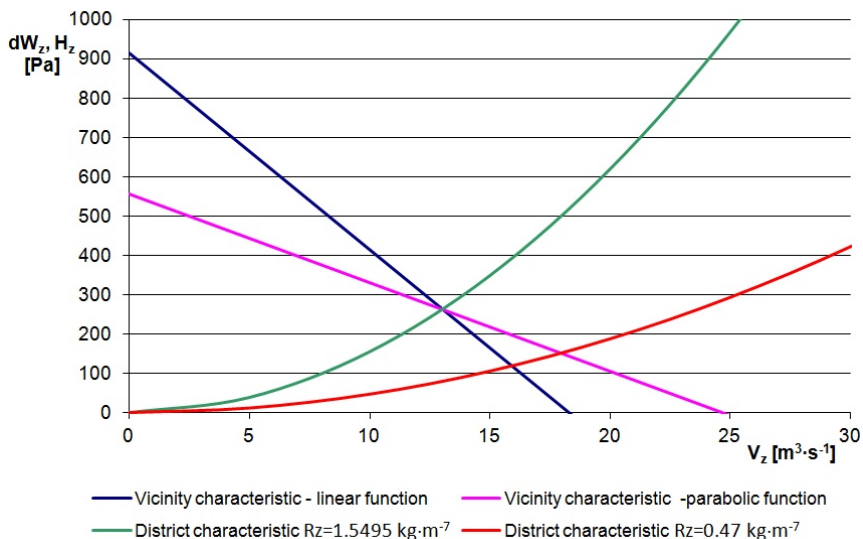


Fig. 6. The characteristics of the vicinity and ventilation district – example 3

of three lines in Fig. 6). Thus, it proves that, taking into consideration the vicinity characteristics, two different ventilation districts with the same values of resistance and air quantities must be treated separately.

5. Conclusions

Giving appropriate consideration to the required air quantity alternative vicinity characteristics of ventilation districts is particularly important (especially when methane and thermal hazards occur). The following conclusions may be drawn:

1. Each district should be considered separately. Even for both identical districts (structure, resistance, air quantity), a change in the branch resistance can produce two different air distributions in the network. This is caused by the different vicinity characteristics (Fig. 6).
2. In contrast to flat vicinity characteristics, steep ones have a smaller influence on the change of air quantity in the district (which are caused by a change of the district resistance) (Fig. 6).
3. In certain cases, the vicinity characteristic can give rise to a situation where a complete opening of the intake stoppings will not produce the required air quantity in the district. This may be a hazardous situation considering methane emissions and thermal hazards (Example 3).

Acknowledgments

Appreciations for Mr. Tim Harrell for English proof reading of the text.

Funding

This research did not receive any specific grant from funding agencies in the public, commercial, or not-for-profit sectors.

References

- Bystróż H., 1956. *Sposób kreślenia kanonicznych schematów przewietrzania*. Przegląd Górnictwa **3**, 86-100.
- Bystróż H., 1999. *Potencjały aerodynamiczne oraz wyznaczanie ich pól w sieciach wentylacyjnych, podsięciach i rejonach*. Archives of Mining Sciences **44** (1), 23-69.
- Cheng G., Qi M., Zhang J., Wang W., Cheng Y., 2012. *Analysis of the Stability of the Ventilation System in Baishan Coalmine*. Procedia Engineering **45**, 311-316. <https://doi.org/10.1016/j.proeng.2012.08.163>
- Drenda J., Sułkowski J., Pach G., Różański Z., Wrona P., 2016. *Two stage assessment of thermal hazard in an underground mine*. Archives of Mining Sciences **61**, 2, 309-322. DOI: <https://doi.org/10.1515/amsc-2016-0023>
- Drenda J., Domagała L., Musioł D., Pach G., Różański Z., 2018. *An analysis of selected jet fans used in chambers of KGHM mines with respect to the air stream range*. Tunnelling and Underground Space Technology **82**, 303-314. <https://doi.org/10.1016/j.tust.2018.08.033>
- Dziurzyński W., Krach A., Pałka T., 2017. *Airflow Sensitivity Assessment Based on Underground Mine Ventilation Systems Modeling*. Energies **10** (10), 1451.

- Gillies A.D.S., Wu H.W., Tuffs N., Sartor T., 2004. *Development of real time airflow monitoring and control system*. Proceedings of the 10th US / North American Mine Ventilation Symposium, Mine Ventilation, Ganguli&Bandopadhyay, Taylor&Francis Group, London 2004. <http://citeseerx.ist.psu.edu/viewdoc/download?doi=10.1.1.610.2435&rep=rep1&type=pdf>
- Hartman H.L., Mutmansky J., Ramani R., Wang Y.J., 1997. *Mine Ventilation and Air Conditioning*. 3rd Edition. New York: John Wiley & Sons.
- Hudeček V., Urban P., Zapletal P., Košňovský V., 2013. *Elimination of safety risks at mined Coal faces in the paskov mine, Staříč plant – OKD, a.s. Czech Republic*. Acta Montanistica Slovaca **18**, 3, 172-179. <http://actamont.tuke.sk/pdf/2013/n3/5hudecek.pdf>
- Jeswiet J., Szekeres A., 2016. *Energy Consumption in Mining Commintion*. The 23nd CIRP Conference on Life Cycle Engineering. Elsevier, Procedia CIRP **48**, 201, 140-145, 2016. doi.org/10.1016/j.procir.2016.03.250
- Knechtel J., 2011. *Thermal hazard prevention in longwalls run under extreme geothermal conditions*. Archives of Mining Sciences **56**, 2, 265-280. <http://archiwum.img-pan.krakow.pl/index.php/AMS/article/view/306/310>
- Kolarczyk M., Oleksy M., Pach G., 2005. *Substitute characteristics of surrounding sub-networks for mining departments in ventilation networks of collieries*. Zeszyty Naukowe Politechniki Śląskiej, seria Górnictwo **270**, 265-276.
- Kolarczyk M., Oleksy M., Pach G., 2006. *Rozwinięcie charakterystyki zastępczej części kopalnianej sieci wentylacyjnej według wzoru Taylora*. Zeszyty Naukowe Politechniki Śląskiej, seria Górnictwo i Geologia **1**, 4, 51-65.
- Kolarczyk M., 1993. *Wpływ struktury kopalnianej sieci wentylacyjnej na wrażliwości prądów powietrza przy zmianach oporów bocznic*. Zeszyty Naukowe Politechniki Śląskiej, z. 214, Gliwice.
- Kolarczyk M., 2008. *The analogy between the conditions concerning airflow outputs sensitivity signs to changes in the resistance of side branches and H. Czeczott's conditions concerning the flow direction in a simple diagonal network*. Archives of Mining Sciences **53**, 2, 270-292. <http://archiwum.img-pan.krakow.pl/index.php/AMS/article/view/539/550>
- Koptoń H., Wierziński K., 2014. *The Balance of Methane and Ventilation as a Tool for Methane Hazard Assessment in the Areas of Longwalls Exploited in Hard Coal Mines*. Journal of Sustainable Mining **13**, 4, 40-46. DOI.org/10.7424/jsm140308
- Krach A., 2014. *Determining Diagonal Branches in Mine Ventilation Networks*. Archives of Mining Sciences **59**, 4, 1097-1105. DOI: <https://doi.org/10.2478/amsc-2014-0076>
- Krause E., Smoliński A., 2013. *Analysis and Assessment of Parameters Shaping Methane Hazard in Longwall Areas*. Journal of Sustainable Mining **12**, 1, 13-19 DOI.org/10.7424/jsm130104
- Liu H., Wu X., Mao S., Li M., Yue J., 2017. *A Time Varying Ventilation and Dust Control Strategy Based on the Temporospatial Characteristics of Dust Dispersion*. Minerals **7** (4) 59. doi:10.3390/min7040059
- Luo W., Xie X., Xiao H., Cui C., Yin X., Su M., Wang T., Li J., Tan X., 2014. *Reliability calculation of mine ventilation network*. Procedia Engineering **84**, 752-757. <https://doi.org/10.1016/j.proeng.2014.10.492>
- Madeja-Strumińska B., Strumiński A., 2004. *Optymalizacja wymuszonych rozplywów powietrza w warunkach skrepowanych oraz ocena wybranych zagrożeń w kopalniach podziemnych*. Oficyna Wydawnicza Politechniki Wrocławskiej, Wrocław. <http://www.dbc.wroc.pl/dlibra/plain-content?id=1006>
- McPherson M., 1993. *Subsurface Ventilation and Environmental Engineering, part two chapter 7 – Ventilation network analysis*. Publisher Springer Netherlands, 209-240.
- Nguyen X.T., Nguyen T.T., Tran D.K., 2009. *Some problems on the research and development of the application of methane draining boring technology to prevent hazards in underground coal mines in Vietnam*. Journal of Coal Science & Engineering. **15**, 2, 129-133. <https://doi.org/10.1007/s12404-009-0203-9>
- Semin M., Levin L., 2019. *Stability of air flows in mine ventilation networks*. Process Safety and Environmental Protection **124**, 167-171.
- Szlązak N., Kubaczka C., 2012. *Impact of coal output concentration on methane emission to longwall faces/Wpływ koncentracji wydobywania na wydzielanie metanu do wyrobisk ścianowych*. Archives of Mining Science **57**, 1, 3-21. DOI: <https://doi.org/10.2478/v10267-012-0001-x>
- Szlązak N., Obracaj D., Borowski M., Swolkień J., Korzec M., 2013. *Monitoring and controlling methane hazard in excavation in hard coal mines*. AGH Journal of Mining and Geoenvironment **37**, 1, 105-116. DOI: <http://dx.doi.org/10.7494/mining.2013.37.1.105>

- Szłazak N., Obracaj D., Korzec M., 2017. *Analysis of connecting a forcing fan to a multiple fan ventilation network of a real-life mine*. *Process Safety and Environmental Protection* **107**, 468-479.
- Szłazak N., Obracaj D., Swolkień J., 2018a. *Sposób postępowania przy projektowaniu eksploatacji pokładów węgla w warunkach zagrożenia metanowego*. *Systemy Wspomagania w Inżynierii Produkcji* **7**, 1, 360-376.
- Szłazak N., Obracaj D., Swolkień J., 2018b. *An Evaluation of the Functioning of Cooling Systems in the Polish Coal Mine Industry*. *Energies* **11** (9), 2267.
- Szłazak N., Obracaj D., Swolkień J., 2019. *Methods of Methane Control in Polish Coal Mines*. In *Proceedings of the 11th International Mine Ventilation Congress* 292-307. Springer.
- Tutak M., Brodny J., 2018. *Analysis of the Impact of Auxiliary Ventilation Equipment on the Distribution and Concentration of Methane in the Tailgate*. *Energies* **11**, 3076, 1-28, doi.org/10.3390/en11113076
- Uzsko M., 2009. *Monitoring of methane and rockburst hazards as a condition of safe coal exploitation in the mines of Kompania Weglowa SA*. *Procedia Earth and Planetary Science* **1**, 1, 54-59, doi.org/10.1016/j.proeps.2009.09.011
- Wang C., Yang S., Li X., Li J., Jian C., 2019. *Comparison of the initial gas desorption and gas-release energy characteristics from tectonically-deformed and primary-undeformed coal*. *Fuel* **238**, 66-74, doi.org/10.1016/j.fuel.2018.10.047
- Wang K., Wu Z., Zhou A., Jiang Y., Feng S., 2016. *Experimental study of high concentrations of coal mine methane behavior in downward ventilated tilted roadways*. *Journal of Wind Engineering and Industrial Aerodynamics* **158**, 69-80.
- Yuan S., Zhang Z., Deng K., Li C., 2010. *Thermal hazard in Chinese coal mines and measures of its control*. *Mine Safety and Efficient Exploitation Facing Challenges of The 21st Century*, p. 15-21.
- Yueze L., Saad A., Agus P.S., Jundika C.K., 2017. *Prediction of air flow, methane, and coal dust dispersion in a room and pillar mining face*. *International Journal of Mining Science and Technology* **27**, 4, 657-662, doi.org/10.1016/j.ijmst.2017.05.019
- Zhong M., Xing W., Weicheng F., Peide L., Baozhi C., 2003. *Airflow optimizing control research based on genetic algorithm during mine fire period*. *Journal of fire sciences* **21** (2), 131-153.